Catal Lett (2009) 128:221–226
DOI 10.1007/s10562-008-9741-9

Adsorption of Formic Acid and its Decomposed Intermediates on (100) Surfaces of Pt and Pd: A Density Functional Study

Clarence M. Y. Yue · Kok Hwa Lim

Received: 3 July 2008 / Accepted: 20 October 2008 / Published online: 21 November 2008

Abstract In this work we have systemically characterized the adsorption of formic acid, its decomposed intermediates and products on the (100) surfaces of Pt and Pd. We observed that adsorbates binding through the C atoms to the surface bind stronger to the Pt surface compared to the Pd surface, while adsorbates binding to the surface via O atoms favor the Pd surface over the Pt surface.

Keywords DFT · Formic acid · Pt · Pd · Adsorption

1 Introduction

As portable and mini-sized electronic gadgets such as cellular phones, Personal Digital Assistants, become more common, unimpressive battery lives become the bane for these devices. Li-ion batteries are unsatisfactory because of their limited power densities. Research is currently headed towards using small-scale fuel cells to power these devices [1].

H_2/air fuel cells are plagued by the problem of high storage cost (i.e. the fuel is a gas) and safety issues (i.e. it is flammable) [1, 2]. Thus, much effort is put into developing direct liquid-feed fuel cells. Recent studies [3–5] have shown that formic acid is the better liquid fuel compared to methanol for the following reasons: (1) severe methanol fuel crossover at modest concentrations (>2 M), while formic acid can be used at concentrations in the range up to about 10 M; (2) comparable power density to a H_2/air fuel cell which also circumvents the problem of hydrogen storage, by virtue of formic acid being a liquid under ambient conditions; (3) under ambient conditions, temperatures $\sim$25 °C, the electro-oxidation of methanol is very sluggish compared to formic acid oxidation [6].

The "ubiquitous" Pt-catalyst or Pt-alloy catalyst have been used widely for Direct Methanol Fuel Cells (DMFCs) and it has been found that Pt–Ru alloy has been the most successful catalyst [6] but not for Direct Formic Acid Fuel Cells (DFAFCs). Instead it has been reported that the Pd-based catalysts give superior performances in DFAFCs [2, 6–8]. Under identical conditions, the power density for Pd-based catalyst is reported to be almost 2–3 times more than that of the Pt or Pt-based alloys catalysts [2, 7]. It is believed that the reaction pathway when using the Pd catalysts proceeds via a more direct pathway to yield CO_2 rather than via the CO route when using Pt catalysts [7].

Most of the studies have been performed on a macroscopic scale, i.e., on pilot scale fuel cells and while this provides useful information, it demonstrates a lack of understanding at the molecular level for two reasons: (1) the better activity of the Pd catalyst is merely quantified in terms of performance parameters like power density; and (2) the mechanism of the decomposition is unclear, and are at best hunches based on past experience. Hence, a computational study, even if it is most likely the "best-case scenario", would provide a better understanding at the molecular level the catalytic reactivity of the Pd and Pt catalysts towards formic acid decomposition process.

In this work, we intend to qualify the reaction energies of plausible reaction pathways occurring on the monometallic surfaces of Pt(100) and Pd(100) by carrying out periodic DFT slab model studies. We first look that the adsorption properties of formic acid and its decomposed intermediates and products. We then try to determine the

C. M. Y. Yue · K. H. Lim (✉)
Division of Chemical and Biomolecular Engineering, School of Chemical and Biomedical Engineering, Nanyang Technological University, 62 Nanyang Drive, Singapore 637459, Singapore
e-mail: kokhwa@ntu.edu.sg

reaction paths of formic acid decomposition by looking at the reaction energies of the possible reaction pathways as illustrated in Fig. 1. This would provide insight to the energetics of the system regarding the preference of CO_2 or CO as the final products in comparison with reported experimental studies carried out in fuel cells. However, in the current work, we have not considered the kinetic aspect of the reaction that may alter the energetic preferences of the pathways due to different reaction barriers.

This work is organized as follows. In Sect. 2, we present and introduce the computational models and methods used in this work. In Sect. 3, we present and discuss the adsorption/binding characteristics of the various intermediate molecular fragments and also the reaction energies of the steps in the proposed reaction network. Finally, in Sect. 4, we will present our conclusions.

2 Computational Methods and Models

Calculations were performed with the plane-wave based Vienna ab initio simulation package (VASP) [9–11] using the PBE generalized-gradient approximation of the exchange-correlation functional [12]. The interaction between atomic cores and electrons was described by the projector augmented wave method [13]. In the calculations of surface models, for integrations over the Brillouin zone, we combined a $3 \times 3 \times 1$ Monkhorst-Pack grid [14]. Throughout we adopted an energy cut-off of 400 eV. Coordinates of adsorbates and substrate atoms included in the optimization procedure were optimized until the forces acting on them were less than 0.1 eV/nm.

Extended surfaces of Pt(100) and Pd(100) were modeled by four-layer slabs. The unit cells consist of nine atoms per layer to enable us to consider surface coverage as low as 1/9. A vacuum spacing of $\sim$1 nm was adopted to separate the periodically repeated slabs. Adsorbates were positioned on one side of the slab for our adsorption studies. For adsorption studies, we studied the adsorption characteristics of formic acid and its the pertinent decomposed intermediates, namely H, O, CO, CO_2, OH, HCOO and COOH on three high symmetrical sites (top, bridge, and hollow) on the Pt(100) and Pd(100) surfaces.

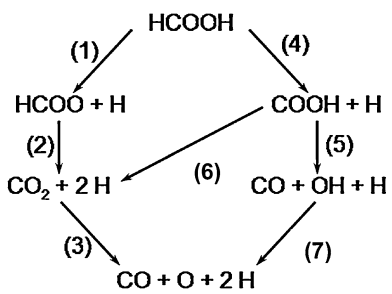

Fig. 1 Reaction network investigated on Pt(100) and Pd(100) surfaces

The binding energy (BE) of an adsorbate is calculated as follows

$$BE = E_{ad/sub} - E_{ad} - E_{sub}$$

where $E_{ad/sub}$ is the total energy of the slab model, covered with the adsorbate in the optimized geometry and E_{ad} and E_{sub} are the total energies of the adsorbate in the gas phase and of the clean substrate, respectively. From this definition, a negative value implies favorable adsorption or release of energy, which is consistent with the conventions adopted in thermodynamics.

The reaction energy of a step in the reaction pathway is calculated as follows

$$\Delta E_{ads} = \Sigma E_{ads(P)} - \Sigma E_{ads(R)}$$

$$E_{gas} = E_{gas(P)} - E_{gas(R)}$$

$$\Delta_{rxn}E = \Delta E_{ads} + \Delta E_{gas}$$

where ΔE_{ads} and ΔE_{gas} are the differences in total energies of the products and reactants in the reaction, for the slab-model and for the gas phase.

3 Results and Discussion

Our calculated bulk optimized Pt and Pd lattice constants are 3.98 and 3.96 Å, in agreement with previous reported result of 3.98 Å [15] and 3.95 Å [16], respectively. Adsorbed complexes of H, O, CO, OH, CO_2, COOH, HCOO, HCOOH on the bulk terminated Pd and Pt (100) surfaces were systemically studied. The most stable adsorption complexes discussed below have been verified by vibrational analysis to be the minima.

3.1 Adsorptions Complexes on Pt(100) and Pd(100) Surfaces

3.1.1 Atomic H

Previous theoretical studies of atomic H adsorption on Pt(111) surface reported binding energies of about -265 kJ mol^{-1} on the top sites and the hollow sites (fcc and hcp) [17, 18] and experimental studies reported a binding energy of -268 kJ mol^{-1} [19]. The results of our current slab model DF calculations (see Table 1) on Pt(100) surface shows that the binding energies at the top, bridge and hollow sites are -262, 282 and -245 kJ mol^{-1}, respectively. The binding energies of our top site agree well with previous reported theoretical [17] and experimental values [19]. While our results showed that the top site is more stable than hollow site, which is in agreement

with previous theoretical study, our most stable site is found to be at the bridge site, which was not reported for the Pt(111) surface.

On Pd(111) surface, previous theoretical study reported binding energies of ~ -220 kJ mol^{-1} (top) and ~ -270 kJ mol^{-1} (hollow) [20], respectively. Our current values of 220 kJ mol^{-1} (top) and -265 kJ mol^{-1} for bridge and hollow sites, respectively, agree very well with the trend and values previously reported despite the differences in surface models and GGA used in the calculations. Here, we observed that H prefers high coordination site on Pd surface, while on the Pt surface, a lower coordination site is preferred. The likely reason that H prefer a lower coordinated site on Pt may be due to its longer lattice constant of 3.98 Å. This makes the hollow site interact less effectively with the H atom as longer H–Pt bonds are envisaged. For atomic H, the largest difference in BE is ~ 50 kJ mol^{-1} and hence makes atomic H very mobile on the metallic surfaces.

3.1.2 Atomic O

Similar to H atom, our DF calculations showed that O atom has essentially no preference for bridge and hollow site with essentially similar binding energy of -400 kJ mol^{-1} on Pt(100) surface while on the Pd(100) surface, atomic O prefers the hollow site with BE values of -404 kJ mol^{-1} in close agreement with previously reported values of ~ -420 kJ mol^{-1} for the Pd(111) surface [20] using the PW91 functional. On the Pt surface, the calculated binding energy value is higher than the reported experimental values of -357 kJ mol^{-1} [21] because of overestimation of the binding energy by the DFT GGA methods. Our calculations showed that on both the Pt and Pd surfaces, the most stable sites is about 100 kJ mol^{-1} more stable than the most unfavorable top site, in good agreement with the trend of previous theoretical calculations on Pt [17] and Pd [20] (111) surfaces.

Here, we observed that although the binding energies of atomic O between the most stable sites and top sites differs by ~ 100 kJ mol^{-1} on Pt(100) and ~ 140 kJ mol^{-1} on Pd(100), the BE difference between the bridge and hollow sites are just 43 and 24 kJ mol^{-1} on Pt(100) and Pd(100) surfaces, respectively. Thus, we would still expect atomic O to be very mobile on the metallic surfaces, although it will tend to avoid the top sites during diffusion on the surface.

3.1.3 Carbon Monoxide (CO)

Optimized geometrical structures showed that CO adsorbed with a perpendicular orientation towards the surface and with C (carbon atom) bound to the metallic surface. Our calculations indicated that there is a preference for CO to bind to the bridge sites on both the Pt(100) and Pd(100) surfaces (with BE values of -197 and -184 kJ mol^{-1} for Pt and Pd, respectively), in good agreement with previously reported values for Pt(111) surface with binding energies of 176 kJ mol^{-1} at the most favorable fcc site [18, 22] and ~ -180 kJ mol^{-1} at the most favorable hollow sites on Pd(111) [20, 23] surface.

Previous calculations based on cluster models for (111) surfaces of Pt_{10} and Pd_{10} reported CO binding energies of 129 and ~ -101 kJ mol^{-1}, respectively [24]. The difference between our current calculated binding energies with the previously reported theoretical calculations is likely because of cluster size effects where only 10 metallic atoms were used. However, the trend of CO binding stronger to Pt surface is reproduced in our current calculations.

3.1.4 Hydroxyl (OH)

The optimized geometry for OH was found to bind in a perpendicular orientation towards the surface with O binding to the Pt(100) surface, but with weaker interactions compared to the Pd(100) surface. We found that OH prefers binding to the bridge site on Pt(100) and Pd(100) with BE of -275 and -261 kJ mol^{-1}, respectively. On both the surfaces, the most stable complexes structure for OH binding to the bridge site is with its H atom tilted. The additional stability is due to the interaction between H and the surface for the titled structure, similar to the case on the top site of Cu(111) surface [25]. On the Pd(100) surface, our binding energy at the most stable bridge site, -261 kJ mol^{-1} agrees well with previously reported theoretical values of -237 kJ mol^{-1} [26]. The differences are due mainly to the different GGA functional used (PW91 vs PBE) and the surfaces (111 vs. 100). Substrate atoms on the more open

Table 1 Calculated BEs (kJ mol^{-1}) for complexes of adsorbates on top, bridge and hollow sites of Pt(100) and Pd(100) surfaces

Adsorbate	Pt(100)			Pd(100)		
	Top	Bridge	Hollow	Top	Bridge	Hollow
H	−262	−282	−245	−220	−265	−265
O	−298	−401	−357	−273	−381	−404
OH	−147	−275	−196	−154	−261	−245
CO	−173	−197	−149	−136	−184	−175
HCOO	−288	−224	−211	−284	−265	−265
$COOH_u$	−254	–[a]	–[a]	−235	–[a]	–[a]
$COOH_d$	−290	−259	−259	−257	−267	−267
HCOOH	−10	−8	−7	−15	−10	−8

[a] Molecule break up after optimization

surface (100 surface) are expected to exhibit enhanced bonding abilities [27]. Here, our results collaborated with this anticipation. Similar to atomic O, the most unstable top site is 128 and 107 kJ mol^{-1} less stable than the most stable sites on Pt(100) and Pd(100) surface, respectively.

3.1.5 Formate (COOH)

Our DF calculations indicated that the most stable structure of $COOH_u$ (H atom tilted upwards) bound to the surface with its C atom on the top site of the metallic surfaces (see Fig. 2). The calculated BE for $COOH_u$ on Pt(100) and Pd(100) are ~ -254 and -235 kJ mol^{-1}, respectively.

However, this molecule is very unstable on the hollow sites of the Pt and Pd surfaces. During geometry optimization starting from the hollow sites, the molecules always break up into CO and OH species where the overall reaction energy is more stable than the adsorbed molecular COOH structure by -19 and -45 kJ mol^{-1} for the Pt(100) and Pd(100) surfaces, respectively.

We have also calculated the configuration with the H atom tilted downwards towards the surface ($COOH_d$). on the top site, his configuration is more stable than the formal configuration by 36 and 22 kJ mol^{-1} on the Pt(100) and Pd(100) surfaces, respectively. This is in agreement with the trend previously observed on Pt(111) surface [18]. Similar to the case of tilting OH, the configuration with H pointing towards the surface allow the attractive interaction between H and the surface and hence increases the binding energy.

3.1.6 Formate (HCOO)

The optimized molecular structure for HCOO preferred to adsorb on the metallic surface in a bridging fashion, i.e. with two O atoms bound to the top sites of two metallic surfaces (see Fig. 2). The corresponding BE values for the most stable adsorption complexes on Pt(100) and Pd(100) were found to be -288 and -284 kJ mol^{-1}, respectively.

Comparing the binding energies of the most stable adsorption complexes of HCOO and COOH, we find that their binding energies are similar (differences are less than 20 kJ mol^{-1}).

3.1.7 Formic Acid (HCOOH) and Carbon dioxide (CO_2)

We found that HCOOH interacts very weakly (BE = ~ -10 to -15 kJ mol^{-1}) with both metallic surfaces, with the BE values an order of magnitude lower than that observed for all other adsorbates studied here. This indicates that the interaction is only a physisorption process. The likely reason is that HCOOH is fully coordinated and the only form of interaction is via the donation of lone pair of electrons from the saturated O atoms. In the same sense,

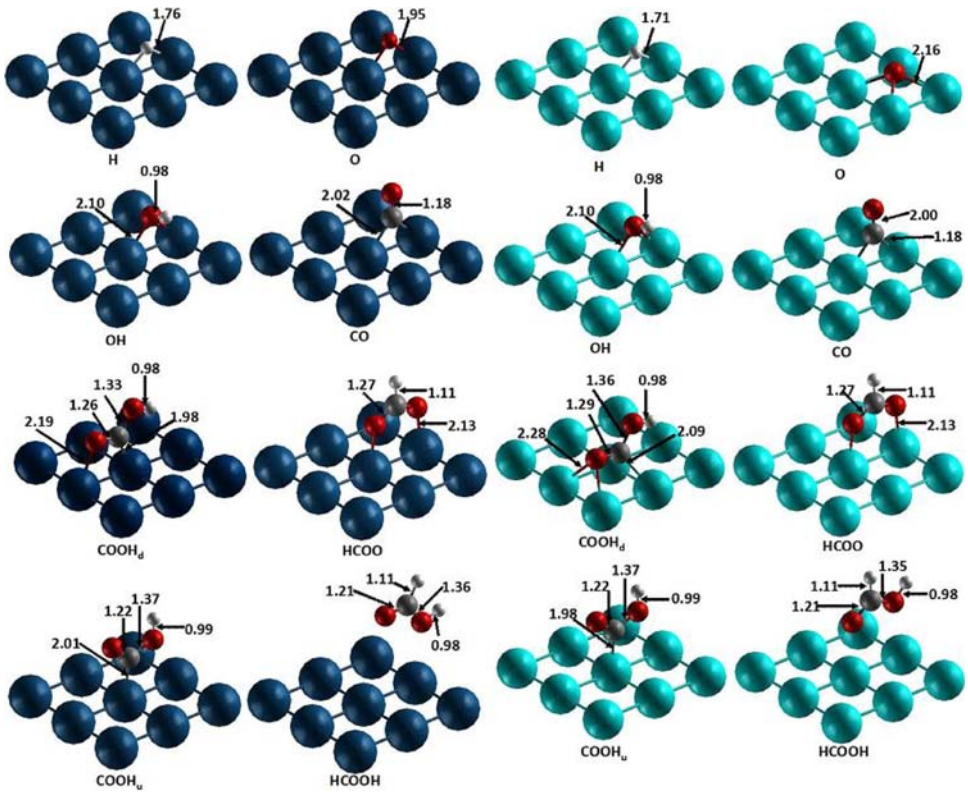

Fig. 2 Side view of the most stable adsorption complexes on (100) surfaces of Pt (*left panel*) and Pd (*right panel*). The pertinent geometric parameters are in Å. *Dark blue sphere*—Pt atom, *light blue*—Pd atom, *dark gray sphere*—C atom, *red sphere*—O atom and *light gray sphere*—H atom

we observed that CO_2 interacts weakly with the Pt and Pd surfaces with essentially zero binding energies.

Our periodic DF slab models calculations for all the adsorbates on Pt and Pd (100) surfaces indicated that their interactions are quite similar with binding energies difference of less than 50 kJ mol^{-1} on all sites. Adsorbates binding through the C atoms bound stronger to the Pt surface compared to the Pd surface, while adsorbates were bounded to the surface via O atoms favored the Pd surface over the Pt surface. We found that HCOOH binds weakly to both Pt and Pd surfaces with binding energies of about 10 kJ mol^{-1} while CO_2 had no propensity to be adsorb on Pt and Pd surfaces with essentially zero binding energies. This is in agreement with experimental report that CO_2 prefers to remain as a free species rather than adsorbed on the metallic surfaces [28].

3.2 Reaction Energies for Proposed Reaction Network for Pt(100) Surface

In Table 2, we reported the reaction energies of various elementary steps for formic acid decomposition as illustrated in Fig. 1. We observed that the reaction step (1), HCOOH → HCOO + H is less favorable than step (4), HCOOH → COOH + H by 43 kJ mol^{-1} on Pt(100) surface, showing that O–H (step 1) bond breaking is less favorable thermodynamically compare to C–H (step 4) bond breaking.

Following step 1, reaction 2, HCOO → CO_2 + H is a moderately exothermic reaction, −38 kJ mol^{-1} and since CO_2 is weakly bounded to the surface, it would likely desorb from the surface rather than under going the mildly exothermic (−28 kJ mol^{-1}) decomposition reaction to CO (step 3). However, if step 4 is followed, step 5 (CO formation) is the probable subsequent path with exothermic reaction energy of −94 kJ mol^{-1} compared to CO_2 formation (step 6) with almost energy neutral reaction energy of −5 kJ mol^{-1}. Overall, thermodynamics would prefer the formation of CO (steps 4 and 5) compare to the formation of CO_2 (steps 1 and 2).

Table 2 Calculated $\Delta_{rxn}E_i$ (kJ mol^{-1}), i = 1–7 for the various steps in the proposed reaction network (Fig. 1) for both Pt(100) and Pd(100) surfaces

Reaction step	Pt(100)	Pd(100)
(1) HCOOH → HCOO + H	−76	−51
(2) HCOO → CO_2 + H	−38	−26
(3) CO_2 → CO + O	−28	−18
(4) HCOOH → COOH + H	−119	−76
(5) COOH → CO + OH	−94	−90
(6) COOH → CO_2 + H	−5	−72
(7) OH → O + H	+72	−1

3.3 Reaction Energies for Proposed Reaction Network for Pd(100) Surface

In contrast to Pt(100) surface, on Pd(100), the cleavage of the O–H bond (step 1) is comparable to C-H bond cleavage, step (4) with difference of 25 kJ mol^{-1}. CO_2 formation, step (1) followed by step (2) is an exothermic reaction, −77 kJ mol^{-1}. Although, the further decomposition of CO_2 to CO (step 3) is almost energy neutral. With essentially zero binding energies of CO_2, it would rather undergoes desorption than further decomposition to CO via step 5 and CO_2 via step 6 are almost comparable thermodynamically.

Here, we conclude that while on the Pt(100) surface, there is a large thermodynamic driving force for CO formation, on the Pd(100), the formation of the final products essentially does not differ too much thermodynamically. Further works to unfold the kinetic factors are required to elucidate the actual reaction pathways for formic acid decomposition process on the Pt and Pd surface and hence to determine the selectivity of the products on the two surfaces.

4 Conclusions

In this work we have systemically characterized the adsorption of formic acid and its decomposed intermediates on the (100) surfaces of Pt and Pd as models for Pt and Pd based catalysts. We observed that adsorbates binding through the C atoms bind stronger to the Pt surface compared to the Pd surface, while adsorbates binds to the surface via O atoms favor the Pd surface to the Pt surface.

We also found comparatively similar values for the adsorption energies for both Pt(100) and Pd(100) surfaces which suggests that their activity for formic acid decomposition are quite similar. Although the reaction energies calculated for the elementary reactions on the surface show that formic acid decomposition may follow different paths, further works is required to obtain the kinetic parameters for these elementary reaction steps are required to conclusively determine that the surface reactions indeed follow different paths on the Pt and Pd surfaces.

Acknowledgements C. M. Y. Yue acknowledges support from NTU URECA's project. This work was supported by NTU's grants SUG 43/06 and M58120000.

References

1. Zhu Y, Ha S, Masel RI (2004) J Power Sources 130:8
2. Miesse CM, Jung WS, Jeong KJ, Lee JK, Lee JY, Han JH, Yoon SP, Nam SW, Lim TH, Hong SA (2006) J Power Sources 162:532
3. Ha S, Larsen R, Zhu Y, Masel RI (2004) Fuel Cells 4:337

4. Rice C, Ha S, Masel RI, Waszczuk P, Wieckowski A, Barnard T (2002) J Power Sources 111:83
5. Ha S, Dunbar Z, Masel RI (2006) J Power Sources 158:129
6. Zhu Y, Khan Z, Masel RI (2005) J Power Sources 139:15
7. Larsen R, Ha S, Zakzeski J, Masel RI (2006) J Power Sources 157:78
8. Lin ZL, Hong L, Tham MP, Lim TH, Jiang HX (2006) J Power Sources 161:831
9. Kresse G, Furthmüller J (1999) Comput Mater Sci 6:15
10. Kresse G, Furthmüller J (1996) Phys Rev B 54:11169
11. Kresse G, Hafner J (1996) Phys Rev B 47:104205
12. Perdew JP, Burke K, Ernzerhof M (1996) Phys Rev Lett 77:3865
13. Kresse G, Joubert D (1999) Phys Rev B 59:1758
14. Monkhorst HJ, Pack JD (1976) Phys Rev B 13:5188
15. Calvo SR, Balbuena PB (2007) Surf Sci 601:4786
16. Taguchi N, Tanaka S, Akita T, Kohyama M, Hori F (2008) Solid State Phenom 139:9
17. Ford DC, Xu Y, Mavrikakis M (2005) Surf Sci 587:159
18. Grabow LC, Gokhale AA, Evans ST, Dumesic JA, Mavrikakis M (2008) J Phys Chem C 112:4608
19. Poelsema B, Mechtersheimer G, Comsa G (1981) Surf Sci 111:519
20. Chen ZX, Neyman KM, Lim KH, Roesch N (2004) Langmuir 20:8068
21. Gland JL, Sexton BA, Fisher GB (1980) Surf Sci 95:587
22. Greeley J, Mavrikakis M (2002) J Am Chem Soc 124:7193
23. Lim KH, Chen ZX, Neyman KM, Roesch N (2006) J Phys Chem B 110:14890
24. Ample F, Curulla D, Fuster F, Clotet A, Ricart JM (2002) Surf Sci 497:139–154
25. Lim KH, Moskaleva LV, Roesch N (2006) Chem Phys Chem 7:1802
26. Cao Y, Chen ZX (2006) Surf Sci 600:4572–4583
27. Chen ZX, Lim KH, Neyman KM, Roesch N (2004) Phys Chem Phys Chem 6:4499
28. Columbia MR, Thiel PA (1994) J Electroanal Chem 369:1